Journal of Catalysis 261 (2009) 34–49

Contents lists available at ScienceDirect

Journal of Catalysis

www.elsevier.com/locate/jcat

Influence of porosity on PE molecular weight from the Phillips Cr/silica catalyst

Max P. McDaniel

Phillips Research Center, Bartlesville, OK 74006, USA

ARTICLE INFO

Article history:
Received 10 August 2008
Revised 30 September 2008
Accepted 28 October 2008
Available online 22 November 2008

Keywords:
Ethylene olymerization
Polyethylene
PE
Molecular weight
Porosity
Polymerization catalyst
Phillips catalyst
Cr/silica catalyst
Chromium polymerization catalyst

ABSTRACT

The porosity of Phillips Cr/silica catalysts plays a major role in determining the molecular weight (MW) and molecular weight distribution obtained during ethylene polymerization. A survey of the many different families of silica was made to evaluate this connection. No one single physical catalyst property, such as surface area, pore volume, radius of curvature, or average pore diameter, could be universally correlated with the MW of polyethylene. Instead the data seem to suggest that the trends observed are the result of two independent influences. First, pore volume determines the fragility of the catalyst, which governs the degree of fragmentation during polymerization, and the fragment size. Secondly, pore diameter controls how easily the polymer can escape from the interior of the fragment. These variables are explored, and possible explanations for the observed behavior are discussed.

1. Introduction

Polyethylene (PE) is the world's most commonly used plastic, and high density polyethylene (HDPE) is the most popular type of PE. Perhaps 40% of HDPE is obtained from the Phillips catalyst, which is usually made by depositing a chromium salt onto a silica gel carrier, followed by calcining [1–3]. Since its discovery in 1951 industrial researchers have noticed that the porosity of the silica carrier can affect the performance of the final catalyst. Predictably, high surface area is necessary to achieve high activity, but high surface area alone is not sufficient. The silica must also be fragile. This is because, once polymerization begins, polymer immediately fills the pores, and they must then rupture for reaction to continue. Otherwise the polymerization quickly stops due to lack of ethylene supply. Thus only high pore volume silicas are fragile enough to fully disintegrate during polymerization.

That porosity should affect the activity of Cr/silica catalysts is thus understandable and the relationship has long been recognized [1,2]. But porosity also influences the character of the polymer produced, and most notably, it controls the molecular weight (MW). Industrial researchers working for both catalyst and polymer manufacturers have been aware of this relationship for five decades and have successfully applied it to many new catalyst variations. However, the reason for this behavior has never been understood, and in fact, no technical hypotheses have even been offered. Little has been published in the scientific literature documenting the principle [2,4,5]. To our knowledge, the earliest public expression of this relationship was a patent issued in 1965 to J.P. Hogan, in which he reports that the average pore diameter of the catalyst controls the MW of resultant polymer [6]. Internal literature at Phillips Petroleum indicates that the principle was known, if not understood, even in the 1950's.

Therefore in this paper we have examined the subject in perhaps more detail than has ever been attempted before. A wide assortment of different silica types was obtained or made, from a variety of different processes, in an attempt to represent varied silica structures. Catalyst was made from each one, and polymer from the catalyst. Molecular weight, MW distribution, and the elasticity of the polymer from long chain branching, were all determined. This paper evaluates the effect of silica porosity on the molecular weight of the resultant polymer. In a following paper we examine the effect of porosity on long chain branching.

2. Experimental

2.1. Catalyst preparation

Silicas were obtained from W.R. Grace or Cabot. Colloidal silicas from Nyacol and W.R. Grace were gelled by neutralizing the pH, and in some cases by adding a trace of Al^{3+} ion. These gels

E-mail address: Max.McDaniel@sbcglobal.net.

0021-9517/$ – see front matter
doi:10.1016/j.jcat.2008.10.015

were either placed in a vacuum oven at 110 °C, or first washed with a large excess of *n*-propanol. Chromium was impregnated to yield 0.35 Cr/nm^2, usually as chromic acetate in methanol. In some cases, where designated, CrO_3 in water was also used as the solvent, such as to impregnate the small-pore molecular sieves. On one pyrogenic silica the Cr was added as *t*-butyl chromate in heptane. On Cabot HS-5 and nanogel, chromyl chloride vapor was deposited from a nitrogen stream, in order to avoid any surface tension at all during drying. As a final step each catalyst was activated in dry air for three hours at 700 °C, unless otherwise stated. They were then stored under dry nitrogen and always protected from contact with the atmosphere. Pore size distributions on the catalyst were always conducted after activation.

2.2. Polymerization

Bench scale polymerization runs were made in a 2.2 L steel reactor equipped with a marine stirrer rotating at 500 rpm. A steel jacket was used to control temperature to within about 0.5 °C, with the help of an electronic control instrument. About 0.05–0.5 g of the solid catalyst was typically tested in 1.2 L of isobutane liquid at 105 °C. Ethylene was then added to the reactor to equal a fixed pressure, normally 550 psig, and maintained there for 1.0 to 1.5 h, so that full activity was reached. After the allotted time, the ethylene flow was stopped and the reactor depressurized and opened to recover a granular polymer, which was then removed and weighed.

2.3. Polymer characterization

In this paper we use the abbreviation "MW" to signify the general concept of molecular weight, and the term M_W to specifically indicate the weight average molecular weight.

Molecular weight and molecular weight distributions were obtained using a PL 220 SEC high temperature chromatography unit (Polymer Laboratories) with trichlorobenzene (TCB) as the solvent, with a flow rate of 1 mL/min at a temperature of 145 °C. BHT (2,6-di-*tert*-butyl-4-methylphenol) at a concentration of 0.5 g/L was used as a stabilizer in the TCB. An injection volume of 200 µL was used with a nominal polymer concentration of 1.5 mg/mL. Dissolution of the sample in stabilized TCB was carried out by heating at 150 °C for 5 h with occasional, gentle agitation. Subsequently, the sample was kept at 130 °C for approximately 18 h (overnight) after which it was reheated to 150 °C for 2 h prior to injection. The columns used were three PLgel Mixed A LS columns (7.8 × 300 mm) and were calibrated with a broad linear polyethylene standard (Phillips Marlex® BHB 5003 resin) for which the molecular weight had been determined using a Dawn EOS multi-angle light scattering detector (Wyatt).

All GPC curves presented here were first normalized, so that the area under the peak represents a fixed weight of polymer. Because of this normalization, anything that broadens the curve will also tend to reduce its height.

3. Results and discussion

3.1. Varying the drying method

The final pore volume of silica is usually determined by the method of drying. That is, silica hydrogel is usually made by neutralizing an acid with sodium silicate solution. Upon reaching a neutral (or at least higher) pH, the colloidal particles suddenly link up into a gel network. In this hydrogel state each gram of silica may contain 2 to 10 g of pore water. In a final step the hydrogel is then dried into a xerogel, in which the pore water is replaced by air. During drying, however, the gel network shrinks due to the high forces of aqueous surface tension on pore walls. The final pore volume (PV) of the silica xerogel may be only 1 mL/g or even less. Usually the surface area (SA), which is typically 200–600 m^2/g, is not affected by the drying step. The process is illustrated in Scheme 1A.

If the pore water is first replaced by an organic liquid, then the drying step does not shrink the network as badly, because the surface tension is greatly diminished. For example, Fig. 1 shows a series of catalysts that were all made from the same silica–titania–chromia hydrogel, containing initially 7 mL/g of pore water. Only the method of drying was varied. At one extreme, the hydrogel was simply placed in a vacuum oven at 110 °C. This caused severe shrinkage, resulting in a final pore volume of only 0.7 mL/g. In the other members of the series, however, the pore water was first replaced with different organics or mixtures of organics and water. Pore volume varied widely, and at the other extreme a final PV of over 3 mL/g was obtained. Surface area was unaffected.

All these xerogels were then calcined and tested for ethylene polymerization. As expected, the activity increased with pore volume, as shown in Fig. 1A, leveling out around PV 2.3–3.0 mL/g. Low PV catalysts are less active because they either possess enough internal strength to resist fragmentation during polymerization, and/or the polymer cannot easily diffuse out of those fragments. Both tendencies result in only a fraction of the total surface area being available for polymer formation.

The weight-average molecular weight (M_W) of the polymer obtained is also plotted in Fig. 1A against pore volume. Notice that M_W decreases with increasing PV also leveling out around 2.3–3.0 mL/g. Also plotted in Fig. 1A is the melt index, which is inversely related to molecular weight. Melt index (or sometimes the high load melt index) is a measure of the flow of the molten polymer under certain specified conditions.[1] Because this test is more easily, and more accurately, carried out in a commercial plant than GPC, it is widely used as surrogate for molecular weight.[2] In this example melt index rises with PV and then also levels out around 2.3 or 3.0 mL/g. The range of melt index, or molecular weight, covered by these changes in PV, is quite significant by industrial standards. Indeed, these methods of drying are used to make many specialty-grade catalysts delivering high melt index or other polymer characteristics.

Given the similar response of activity to PV, it is tempting to attribute the MW change to localized overheating from the more active catalysts. Molecular weight is known to be decreased by higher reactor temperature, which is one of the main industrial control mechanisms used for fine tuning. However, other cases are described below where MW did not parallel the overall activity of the catalyst. For example, increasing the surface area can increase the activity, but not always accompanied by decreased MW. So some other explanation for the dependence of MW on PV must be sought.

Since the surface area did not change in this series, the average pore diameter must increase with increasing PV. In fact the average pore diameter is usually expressed by the following equation, which derives from the geometry of an open cylinder:

$$\text{average pore diameter} = 4(\text{pore volume})/\text{surface area}.$$

The increase in pore diameter in this series is also shown in Fig. 1B, where nitrogen sorption is plotted against pore diame-

[1] Melt index (MI) in grams of polymer per 10 min was determined in accordance with ASTM D1238-E, condition 190/2, at 190 °C, with a 2160 g weight, 190 °C. High load melt index (HLMI, g/10 min) was determined in accordance with ASTM D1238-F, condition 190/21.6, at 190 °C with a 21,600 g weight.

[2] Melt index is also influenced by MW breadth and long chain branching. Therefore melt index only serves as a substitute for MW when these other factors do not change significantly, as is usually the case.

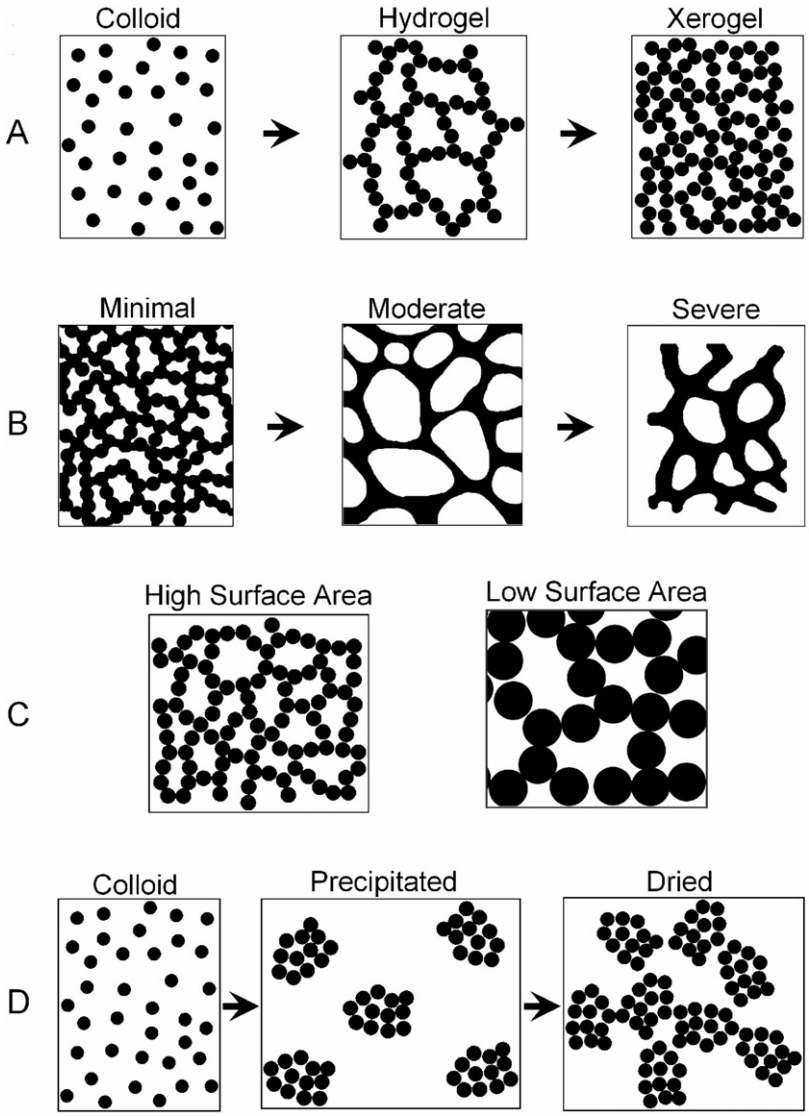

Scheme 1. Silica structures. (A) Primary silica particles in a colloidal sol link into chains to form a gel network that shrinks to varying degrees during drying depending on the surface tension of the solvent. (B) Coalescence of silica gel, resulting in loss of surface area, pore size expansion, lower pore volume, and a change from convex to concave pore surface. (C) Colloids provide non-reinforced gels of varying surface area. (D) Morphology of precipitated silica.

ter. Notice that as the pore volume increases (the area under each curve), so does the pore diameter. Thus the data in Fig. 1A can also be plotted as a function of the pore diameter and this is the second X-axis shown at the top of the graph. Whether the increasing melt index is attributed to expanding pore diameter, as Hogan [6] did, or to pore volume itself, or perhaps to some other derivative factor, cannot be discerned from this data alone, but the subject will be discussed further below.

3.2. Mass transport

One idea that first comes to mind when contemplating the effect of porosity is ethylene transport through the pore structure. One might imagine that ethylene supply would be more limited to sites existing inside a small pore structure. Alternatively, small pore silicas might fracture into larger fragments than weaker, large pore silicas, thus also limiting their access to ethylene. This is in agreement with the observed activity dependence on porosity, as shown in Fig. 1A. Unfortunately this idea actually runs contrary to the known dependence of M_W on ethylene concentration [1,7]. Melt index goes up, not down, as the ethylene concentration is deliberately lowered. This is caused by chain transfer to Cr, as explained elsewhere [1,2].

There is another objection to the idea of mass transport being the determining connection between MW and porosity. By this reasoning one might expect the different PE processes to respond differently. That is, the M_W of polymers made in a slurry system, as in Fig. 1A, might be expected to have a different dependence on porosity compared to polymers made in a gas phase system, where diffusion should be more rapid, or in a solution system, where the polymer dissolves away from the catalyst as it is formed. Yet the M_W dependence on porosity exists in all three processes.

Table 1 presents an example of the M_W dependence in the solution process. Here the Cr/silica catalysts of varying porosity were activated at low temperature (540 °C) and the reactor temperature was set at 146 °C using cyclohexane solvent, well above the temperature at which PE goes into solution. Yet one can see the same dependence of melt index on porosity. In this example, where both PV and SA were simultaneously varied, it seems that the correlation works better with the pore diameter itself, as Hogan proposed, rather than the pore volume.

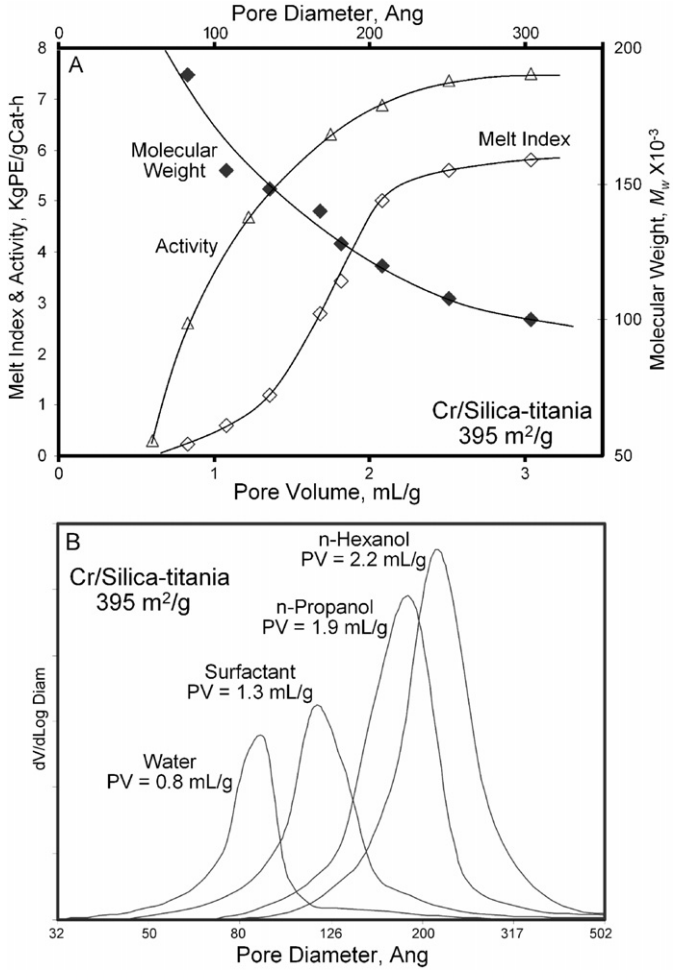

Fig. 1. Drying hydrogel from different solvents yields catalysts of constant surface area but varying in pore volume and pore size. (A) Activity, melt index and M_W response to catalyst pore volume. (B) Pore volume distribution of a few samples dried from various liquids.

Table 1
Melt index varies with porosity even in a solution polymerization.

Surface area (m^2/g)	Pore volume (mL/g)	Avg. pore diameter (Å)	Melt index (g/10 min)
736	0.65	35	0.21
639	0.90	56	0.28
566	0.95	67	0.29
744	1.16	62	0.40
418	0.95	91	0.73
256	1.20	188	1.50
265	2.30	347	2.70

Cr/silica 540 °C, Rxn 146 °C, 450 psig.

3.3. Dehydroxylation vs pore diameter

One possible explanation is that porosity influences dehydroxylation during calcining. The activation temperature is a major variable that controls MW. Higher temperatures cause greater dehydroxylation and annealing, which in turn results in higher melt index (lower M_W) [1,2]. This relationship is shown in Fig. 2. At first it is not obvious how porosity and dehydroxylation could be related. However, there are a few silica studies that could indicate a connection [8–12]. Large pore silicas were found to thermally dehydroxylate more easily than those containing smaller pores. The phenomenon was attributed to (1) more hydrogen bonding between silanols in the more negative radius of curvature within

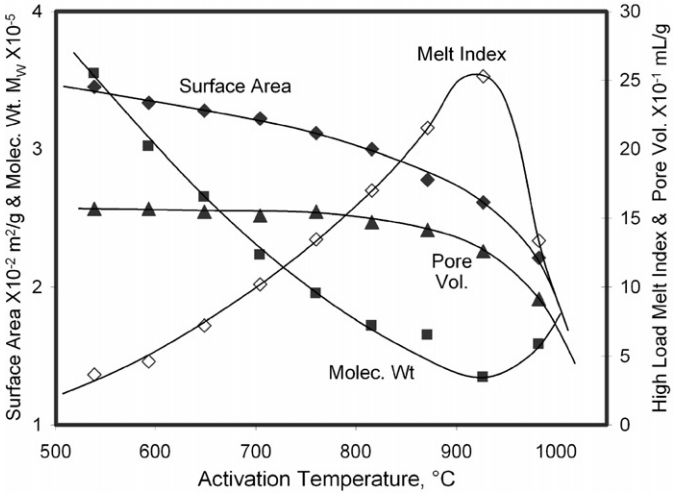

Fig. 2. Effect of activation temperature on melt index and molecular weight.

narrow pores, perhaps near the point of contact between primary particles, and (2) greater difficulty of diffusing moisture out of small pores during calcining. Whatever the underlying explanation for the difference in dehydroxylation, the idea correctly predicts the direction of change in MW.[3] That is, catalysts with low PV (smaller pores) should dehydroxylate less efficiently, and therefore resemble a catalyst calcined at lower temperatures, producing lower melt index. The idea also correctly predicts that the relationship should apply to slurry, gas phase, and solution processes alike.

To test this idea another experiment was conducted. In a reversal of the treatment in Fig. 1, a high pore volume dry catalyst (PV = 3.3 mL/g) was placed in a press and compacted under varying pressures up to 70,000 psig. This crushed the pores to different degrees, creating a pellet that was then ground into a 100–200 micron powder, yielding pore volumes that varied widely with applied pressure. These catalysts were activated at 700 °C. The PV distributions from these catalysts are shown in Fig. 3A, and the summary data is listed in Table 2. Notice that PV decreases with compressive force applied, and the pore diameter also decreases. Surface area, as would be expected, remained constant. For comparison, one sample shown in Table 2 was not compacted, but instead was simply wet with water and then dried, to cause shrinkage in another way. It also provided a low PV catalyst but the PV distribution was a little narrower than those formed by compaction.

After activation, these catalysts were then allowed to polymerize ethylene at 105 °C in the usual way. As in Fig. 1, activity declined with pore volume, as shown in Fig. 4A. The melt index also decreased with lowered PV. In fact the melt index and M_W dependence, which are plotted in Fig. 4B against PV, appear to be the same response seen in Fig. 1. Thus it seems that the method of varying the PV is not limited to the drying technique. Melt index varies with pore volume, even in this dry-compacted series. The activity also varied with PV, and when plotted yielded a curve like that in Fig. 1.

The dry compression technique then presents an opportunity to test the hypothesis that large pores dehydroxylate more readily. Some of the catalysts in Fig. 4 and Table 2 were compacted before calcining, while others were compacted after calcining. The calcined catalysts required more pressure to reach similar levels of compaction, indicating greater strength. Both series were tested

[3] But it does not predict the direction of the elasticity change, which is described in the following paper in this series.

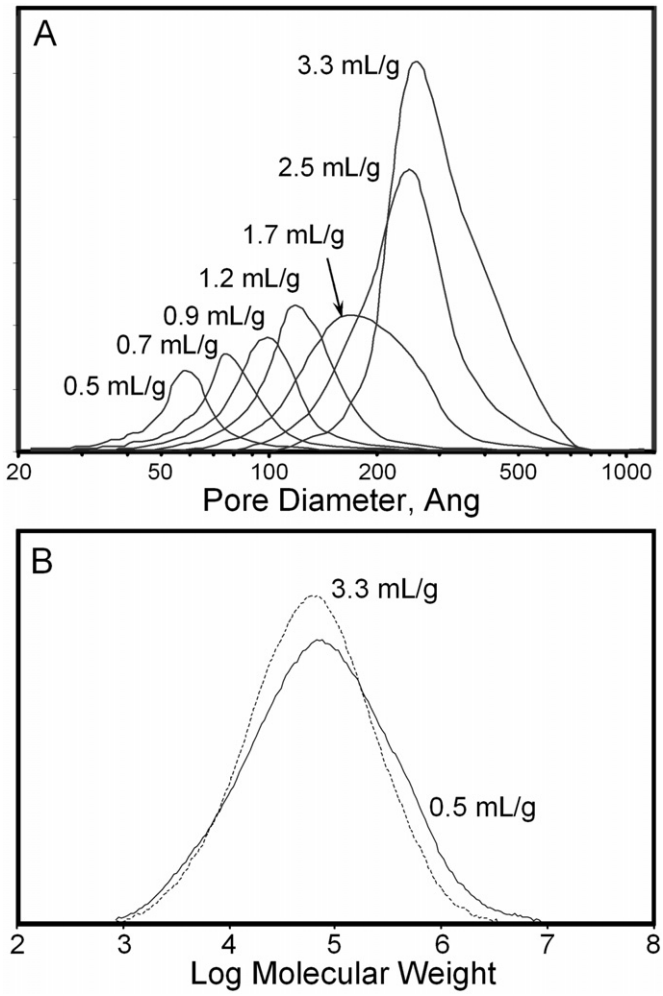

Fig. 3. Effect of compacting Cr/silica–titania catalyst: (A) pore volume distributions and (B) MW distribution of two polymers representing the extremes in the series.

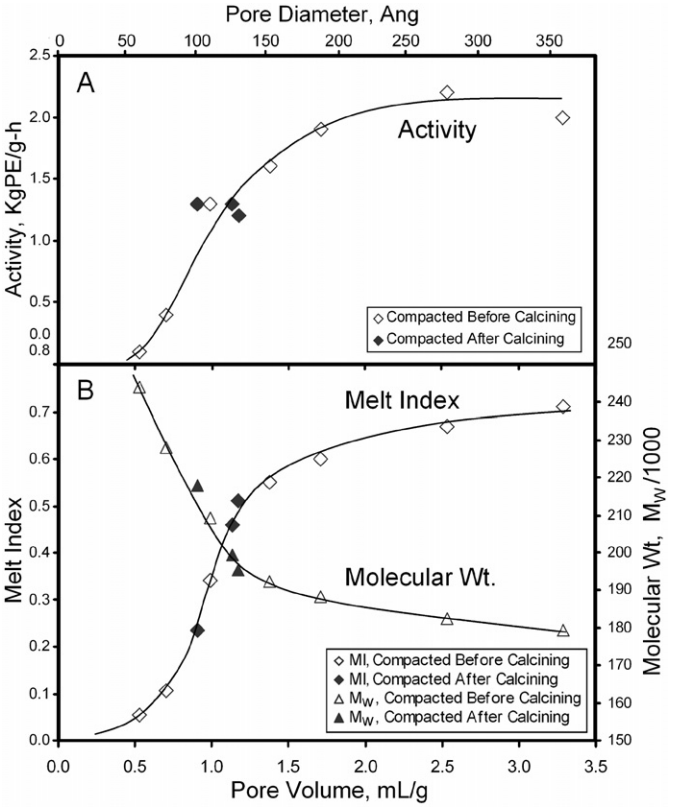

Fig. 4. Effect of compacting Cr/silica–titania catalyst. Surface area was constant at about 365 m^2/g while pore volume was varied through applied pressure. (A) Activity and (B) molecular weight and melt index, both plotted against pore volume and pore diameter.

for polymerization and the results are shown in Fig. 4 and Table 2. Notice that they define one single line. Compaction had the same result whether conducted before or after calcining. Therefore, one cannot invoke diminished dehydroxylation as the cause when the catalysts were compacted *after* calcining. The reason behind the relationship between PV and M_W must be attributed to some other mechanism.

Fig. 3B shows the change in MW distribution that was obtained by compacting the catalyst. The two extremes of the series are shown, from highest to lowest pore volume. A shoulder developed on the high MW side of the distribution when the pores were compressed. This will be discussed more below. The two curves, and in MW distribution curves to be shown later, were both normalized so that the area under the curve represents a fixed weight of polymer. Therefore anything that broadens the peak will also tend to reduce the peak height. One can see this effect in Fig. 3B.

3.4. Alkaline aging

One widely used method of controlling porosity is to "reinforce" the silica network by alkaline aging. Once formed the hydrogel is treated in alkaline solution at 70–100 °C and pH 9–12 for several hours. This causes small amounts of silica to be partially dissolved and re-deposited at the points where primary particles contact [5,7,13–16]. Called "Oswald ripening," the result is a fusion of primary particles together, with loss of the fine structure of the matrix, and consequent reduction in surface area. The over-

Table 2
Effect of compacting Cr/silica–titania in a press.

Compacted before or after calcining	Compaction pressure (Kpsig)	Surface area (m^2/g)	Pore volume (g/mL)	Pore diameter (Å)	Activity (KgPE/g-h)	Melt index (g/10 min)	Molecular weight (M_W/1000)
Before	0	364	3.29	361	2.0	0.71	179
Before	5	366	2.53	277	2.2	0.67	183
Before	10	362	1.71	189	1.9	0.60	188
Before	14	365	1.38	151	1.6	0.55	192
Before	48	363	0.70	77	0.4	0.11	228
Before	55	358	0.53	59	0.1	0.06	244
After	48	354	1.13	128	1.3	0.46	200
After	48	361	1.18	130	1.2	0.51	195
After	70	345	0.91	105	1.3	0.23	218
Before (H_2O, Dry)	0	372	0.99	106	1.3	0.34	209

Table 3
Alkaline aging hydrogel to lower the surface area.

Aging time (h)	Surface area (m^2/g)	Pore volume (mL/g)	Avg. pore diameter (Å)	Activity (gPE/m^2-h)	Melt index HLMI (g/10 min)	Molecular weight (M_W/1000)
0	452	1.96	173	9.3	11	230
1	424	1.91	180	11.1	15	207
4	395	1.85	187	13.2	14	205
12	373	1.90	204	15.3	20	185
20	351	1.88	214	18.2	23	177
28	335	1.99	237	20.3	26	169

Cr/silica–titania, 800 °C.

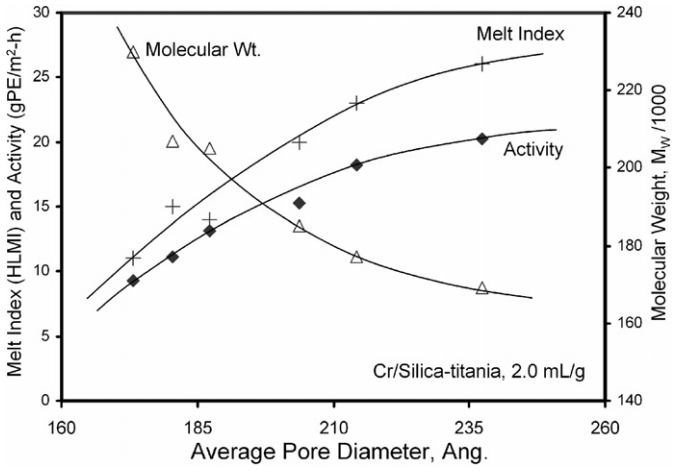

Fig. 5. Effect of varying surface area while holding pore volume constant. Silica–titania hydrogel samples were alkaline aged to lower the surface area, yielding a range of pore sizes all at about 2 mL/g.

all volume of the hydrogel network may not change greatly, if the aging step is not too severe. Scheme 1B shows an illustration of this process. Extreme aging, however, can cause major shrinkage of the hydrogel network itself. That is, both PV and SA are lost. The "neck" regions, where primary particles contact, tend to grow, so that upon drying these "reinforced" gel networks are often better able withstand shrinkage. The final dry pore volume can be unchanged, or even increased, if the treatment is not too severe. Scheme 1B also shows how the radius of curvature of the silica surface can transform from highly convex, to concave.

Alkaline aging provides an opportunity to vary the pore diameter without changing the pore volume itself, thus separating the two variables. In another series of experiments a silica–titania–chromia hydrogel was alkaline aged at 80 °C for times ranging from 0 to 28 h. Then each sample was washed in *n*-propanol and dried, followed by activation at 800 °C. The physical properties are listed in Table 3. Notice that the surface area dropped significantly with aging time, while the pore volume remained constant. Therefore the pore diameter was increasing with aging time.

The results of polymerization tests are also listed in Table 3, and they are plotted in Fig. 5. To take into account the different surface areas of each catalyst, the activity in this series is given per square meter of surface, in order to normalize it. Notice that the activity increased with pore diameter, seeming to level out at 200–300 Å, as also in Figs. 1 and 4. Since the PV was constantly high in this series, it is more difficult to attribute this response to the fragility of the catalyst network, i.e. that small pores result in larger fragments. Instead it could also be interpreted to mean that the surface within the fragments may become more available with increasing pore diameter. That is, the larger diameter may help polymer to escape, thus resulting in greater utilization of the surface *within* each fragment.

Table 4
Some commercial silica gels formed by varying degrees of alkaline aging.

Silica grade	Surface area (m^2/g)	Pore volume (mL/g)	Pore diameter (Å)	Activity (gPE/m^2-h)	Molecular weight (M_W/1000)
W.R. Grace silicas					
Grade 951	602	1.00	67	4.8	433
Experimental	723	1.98	110	5.5	283
Grade HA30W	517	1.42	110	5.6	295
Grade Syloid 244	300	1.50	200	7.3	213
Grade 969MPI	280	1.60	242	7.9	201
Grade 969ID	280	1.30	186	7.1	242
Grade LSA 969MS	237	1.75	296	8.0	200
Grade 250A Carrier	180	1.15	256	8.3	224
Grade 350A Carrier	134	1.23	367	10.0	240
Grade 1000A	33	0.62	742	5.2	410
Other silicas					
Cabot nanogel	801	5.52	276	6.9	217
CPC Acid 1	1709	1.08	25	0.9	494
CPC Acid 2	1055	1.02	39	1.8	450

In Fig. 5 melt index increases, and molecular weight decreases, with expanding pore diameter, both leveling out at 200–300 Å, as was also observed in Figs. 1 and 4. In this series it is pore diameter, as Hogan chose, and not pore volume, that correlates with the polymer. One could also argue that surface area correlates with molecular weight in this study, although this did not hold up in other studies below.

Once again it is tempting to correlate the MW response to the changing activity. That is, localized overheating from the more active catalysts also lowers the molecular weight. In this case, however, the activity is expressed per square meter of surface. By this reasoning, any variable that changes the activity should also affect the molecular weight. However, this general rule does not universally hold. Adding poisons, for example, or simply lowering the Cr loading, influences activity but does not cause the expected molecular change.

3.5. Commercial catalysts

In fact alkaline aging is a common industrial method of manufacturing silicas of different surface area and pore size. Typically a parent hydrogel is made having a surface area of about 800–1000 m^2/g. After minimal aging, and upon spray drying, it produces a material of about 600–700 m^2/g and up to 1 mL/g. However, other grades of lower surface area can be made from the same hydrogel by giving it an increasingly severe alkaline aging treatment (pH, temperature, time), followed by spray-, tray-, or flash-drying. Surface area can be varied down to 35 m^2/g.

Table 4 lists a few examples of commercial silicas made in this way. In the upper series, which were W.R. Grace silicas all made from a similar parent hydrogel, the surface area was lowered (going down the table) over an order of magnitude by increasingly severe alkaline aging. The final PV also varied somewhat because the drying methods were different. Many grades were spray dried, others pan dried, and one (labeled "Experimental") was even dried by organic extraction. Five members of this series are actual commercial catalyst grades that are widely used. Those with very low surface area are silicas designed for chromatography. Like the series in Fig. 5, most of the increase in pore diameter in this series is due to lowered SA and less to a change in PV.

Besides the W.R. Grace silicas, some other related gels are also shown in lower Table 4, to illustrate the extremes in pore volume and surface area. A sample from Cabot, called "nanogel," was made by special drying techniques conducted near the critical point of the solvent, where surface tension approaches zero. It had a pore volume of over 5 mL/g!

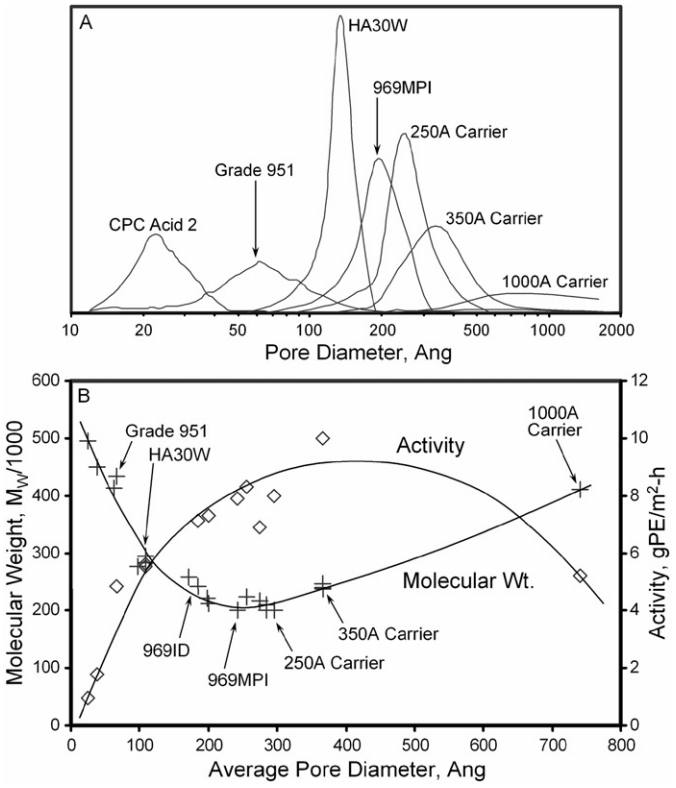

Fig. 6. W.R. Grace silicas made from a similar hydrogel parent to yield varying degrees of coalescence, and pore diameter. (A) Pore volume distributions and (B) M_W and activity response to average pore diameter.

Fig. 6A shows the PV distribution from some of these silicas, which in each case was a single Gaussian peak. One can see in the figure how the pore size varies over a wide range, while the pore volume (the area of each peak) does not change so much. Catalysts were made from these grades by adding 0.35 Cr/nm^2, followed by activation at 700 °C, and the polymerization testing at 105 °C. The activity obtained is reported in Table 4 and plotted in Fig. 6B, again normalized by surface area. Expressed in this way, the activity rises with increasing pore diameter, similar to that in Fig. 5. It flattens out in the 200–300 Å range, and eventually seems to drop under extreme coalescence at 750 Å (the 100A Carrier). Although the PV was moderate during the entire series, the 1000A Carrier had a low PV and this may have contributed to its lower activity.

The M_W of the polymers is also listed in Table 4. This time it does not correlate very well with pore volume, but as Hogan noted, it does seem to correlate with pore diameter, which is plotted in Fig. 6B. Notice that the molecular weight in Fig. 6B decreases with increasing pore diameter in the 0 to 200 Å range, as it did in Figs. 1A and 4B where the surface area was held constant. In Fig. 6B, however, only a small part of this response came from an increasing pore volume. Mostly it results from diminishing surface area, which increases the pore size, as in Fig. 5 where the PV was constant. Thus one could just as well have plotted M_W against surface area in Fig. 5, and also within this series. However, the correlation with surface area is not quite as good here because of the different drying methods used and consequent pore volumes. The pore diameter, which is the ratio 4PV/SA, seems to help take these variations into account.

In Fig. 1 the melt index (or molecular weight) levels out after a pore diameter of about 200–250 Å is reached. After that point the melt index (or M_W) remains fairly constant. In Fig. 6B the molecular weight also reaches a low point at around 200–300 Å. The 1000A Carrier, where extreme aging produced a very large pore diameter of 750 Å, gave an increase the molecular weight again so that M_W goes through a minimum at around 200–300 Å diameter. The reason for this increase in M_W at very large diameter is unclear, but it seems to occur when the silica network becomes highly reinforced with low PV, perhaps resisting disintegration during polymerization and producing larger fragments.

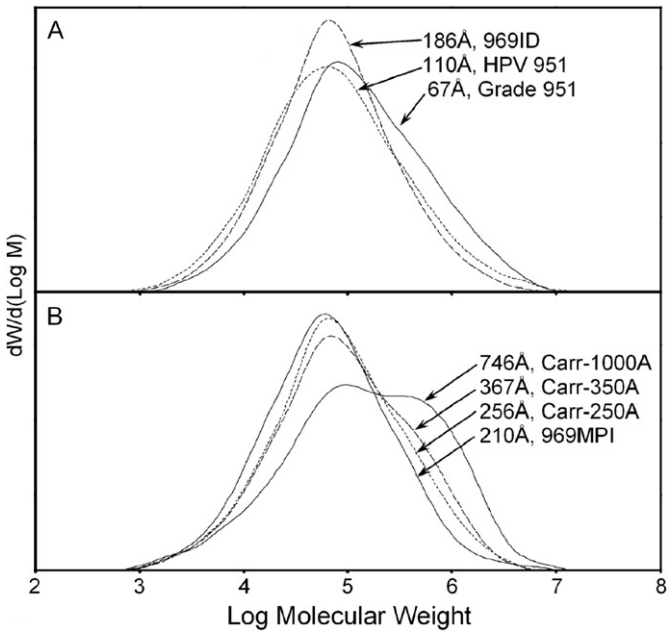

Fig. 7. MW distribution from W.R. Grace silicas: (A) small pore silicas and (B) large pore silicas.

The molecular weight distribution was also affected by the porosity of the silica. Some examples from this series are shown in Fig. 7. In Fig. 7A are the MW distributions from the small pore catalysts, and in Fig. 7B are those from large pore catalysts. Notice that those with average pore diameter around 200–300 Å produce a single peak centered at about MW = $10^{4.8}$ under these reaction conditions. However, for silicas having extremely large or small pores the MW distribution broadens on the high MW side as a shoulder or even a second peak at around MW = $10^{5.8}$ is added. The meaning of this second peak is will be discussed below.

3.6. Thermal sintering

As the activation temperature of Cr/silica is increased, dehydroxylation and annealing are enhanced, and the melt index potential of the catalyst also increases [1,2]. An example of this was shown in Fig. 2, where melt index, M_W, SA and PV are all plotted against activation temperature for a typical Cr/silica catalyst. Notice that the trend reverses at about 900 °C where sintering begins. Sintering is just the earliest stage of melting, and again surface area is lost due to coalescence of primary particles. Pore volume can also decrease significantly. The result is an increase in average pore diameter. It is this physical change in the silica structure that causes the downturn in melt index, and not any chemical change to the chromium. This can be easily demonstrated by sintering the silica alone first. Then the surface can be rehydrated by soaking it in liquid water for some days, followed by chromium impregnation, and then another activation at milder temperatures. It now produces a lower melt index than the virgin Cr/silica catalyst.

Some examples of this are plotted in Fig. 8, and summarized in Table 5. Two silicas were obtained from W.R. Grace as grade 951 (600 m^2/g, 1.0 mL/g) and grade 952 (300 m^2/g, 1.6 mL/g). Both are derived from a similar parent hydrogel, varying mainly in the degree of alkaline aging each grade is subjected to. In one ex-

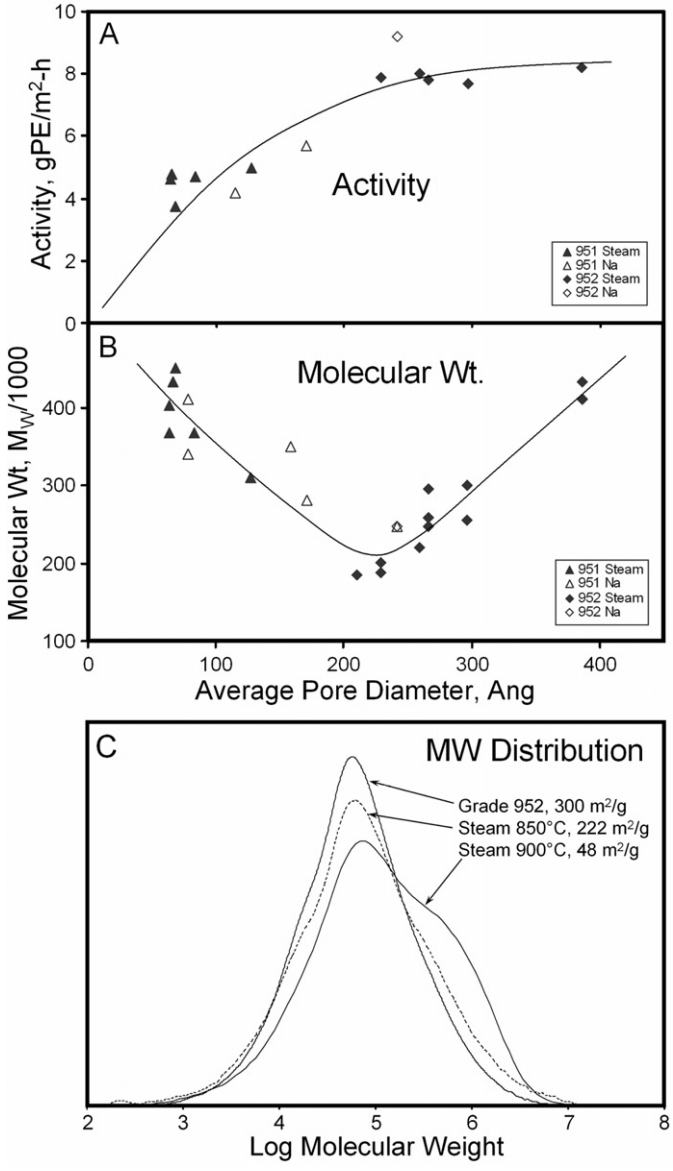

Fig. 8. Catalysts made by sintering two grades of W.R. Grace silica. (A) Activity and (B) molecular weight, both plotted against the average pore diameter. (C) Molecular weight distribution from sintered catalysts made from grade 952 silica, showing the extremes in the series.

periment these silicas were steam-treated at 700–900 °C to cause varying degrees of sintering [8]. Then they were soaked in liquid water for 24 h, followed by impregnation of chromium acetate, and activation at 700 °C in dry air. In some cases the surface area dropped to a small fraction of its initial value, indicating a high degree of coalescence of the fine structure. Pore diameter increased in every case, even when some loss of pore volume was observed.

In a second series of experiments these same two silica grades were sintered in a different way. A small amount of sodium salt (0.3 mmol/g) was impregnated onto silica samples. Sodium ions are known to act as a flux, catalyzing the making and breaking of Si–O–Si bonds during subsequent calcining steps at 700–800 °C [15,17,18]. This treatment reduced the surface area significantly. Then the sodium was washed off of each silica sample, simultaneously rehydroxylating the surface, and chromium was applied from aqueous solution. A final activation at 700 °C resulted in catalysts that again varied in the level of surface area loss, and therefore in average pore size. Both grades 951 and 952 were tested in this way. These results are also summarized in Table 5 and Fig. 8.

Activities, plotted in Fig. 8A, were once more adjusted for surface area and given per square meter of surface. There is again a movement to higher yields as the pore diameter increased. In both series major sintering, even resulting in large PV loss, did not dampen the activity, which suggests that polymer escape from (possibly larger) fragments is promoted by the larger pore diameter.

The molecular weight is plotted in Fig. 8B against pore diameter. One sees the same trend that was observed in Fig. 6B. Molecular weight went through a minimum at around 200–300 Å. The rise in MW at larger diameters was possibly more rapid than in Fig. 6B. This may be a secondary effect from the lower PV obtained in this series.

In this study the change in pore diameter is due to the coalescence of fine structure, mainly resulting in loss of surface area. Thus one could also plot M_W against surface area as an indicator of fusion. This gives two independent and intersecting lines, presumably because of the different starting pore volume in each series. The grade 951 line declines with increasing coalescence, whereas the grade 952 line rises. In contrast, the pore diameter, which is related to the ratio PV/SA ratio, seems to help take these variations into account and unify the two series into a single trend. Again the best correlation seems to be with pore diameter.

Fig. 8C shows that such sintering also affected the MW distribution in much the same way as observed in Fig. 7. Notice that a shoulder is introduced onto the high MW side of the MW distribution when the pore size becomes very small or very large.

Table 5
Results from thermally sintered silicas.

Silica grade W.R. Grace	Treatment	Surface area (m^2/g)	Pore volume (mL/g)	Avg. pore diameter (Å)	Activity (gPE/m^2-h)	Molecular weight ($M_w/1000$)
951	None	602	0.98	65	4.8	465
951	Steam 850 °C 3 h	544	0.93	68	3.7	450
951	Steam 900 °C 3 h	470	0.85	64	4.6	403
951	Steam 950 °C 3 h	394	0.82	83	4.7	367
951	Na 750 °C	249	0.71	114	4.2	340
951	Steam 950 °C 6 h	148	0.48	128	5.0	310
951	Na 800 °C	142	0.60	171	5.7	281
952	None	280	1.60	229	7.9	185
952	Steam 750 °C 3 h	235	1.53	259	8.0	234
952	Steam 800 °C 3 h	228	1.69	297	7.7	284
952	Steam 850 °C 3 h	222	1.48	266	7.8	275
952	Na 750 °C	177	1.07	242	9.2	313
952	Steam 900 °C 3 h	49	0.48	386	8.2	387

Table 6
Results from colloidal silicas converted into solid supports by gelation or precipitation.

Primary particle size	Treatment	Surface area (m^2/g)	Pore volume (mL/g)	Avg. pore diameter (Å)	Melt index (HLMI)	Activity (gPE/m^2-h)	Molecular weight ($M_w/1000$)
7 nm	Gelled, dried from IPA	323	1.59	197	63.5	6.1	136
7 nm	Dried from water	299	0.69	93	9.1	2.1	238
7 nm	Precipitated & dried from IPA	300	1.00/0.27	36	1.6	2.4	326
12 nm	Gelled, dried from IPA	218	1.01	186	44.5	4.7	163
12 nm	Gelled, dried from water	233	0.53	91	4.1	2.0	238
12 nm	Precipitated & dried from IPA	220	0.87/0.16	32	1.2	1.9	306
17 nm	Gelled, dried from IPA	164	0.74	180	26.3	5.7	176
17 nm	Dried from water	161	0.47	116	9.4	1.9	201
20 nm	Gelled at 20%, dried from IPA	138	1.20	349	24.8	4.9	172
20 nm	Gelled at 40%, dried from IPA	136	0.68	202	21.6	3.6	172
20 nm	Gelled at 10%, dried from IPA	137	0.64	185	16.0	2.5	206
20 nm	Gelled at 40%, dried from IPA	149	0.49	131	10.0	2.6	218
20 nm	Gelled at 40%, dried from IPA	133	0.48	143	13.4	2.2	178
20 nm	Dried from water	128	0.46	150	6.5	2.2	183
20 nm	Precipitated & dried from IPA	135	0.67/0.34	100	3.3	2.1	232
20 nm	Precipitated, NH_4OH aged & dried	132	0.60/0.46	139	12.7	2.2	211
50 nm	Gelled, MeOH, iC4 critical pt	103	1.27	495	30.7	6.6	176
50 nm	Gelled, MeOH, iC4 critical pt	92	1.03	447	20.4	6.5	193
50 nm	Gelled, dried from IPA	62	0.56	364	6.3	3.1	250
85 nm	Gelled, dried from IPA	43	0.53	497	9.2	3.5	192
85 nm	Dried from water	43	0.22	256	2.6	2.3	271
85 nm	Precipitated & dried from IPA	35	0.43/0.10	114	0.3	2.0	467

Note. IPA = isopropyl alcohol.

3.7. Varying the primary particle size

Stable colloidal suspensions, containing between 20 and 40% silica, are made commercially through ion exchange by W.R. Grace or Nyacol in which the particle diameter can be controlled from 7 to 85 nm. These colloidal particles can then be gelled or precipitated by adjusting the pH or ionic environment of the suspension. In this way silicas may be formed structure. This is illustrated in Scheme 1C. These colloids provide an opportunity to study the effects of surface area, and radius of curvature, without reinforcement of the structure by coalescence from alkaline aging or sintering.

Therefore silica samples were made from these colloidal suspensions in which the surface area was varied from 300 down to 35 m^2/g, by choosing widely different sizes of the colloidal primary particle. Different drying methods were also applied in order vary the pore volume. However, the structure should not have varied, since all samples were formed by the coagulation of variously sized, non-porous, colloidal silica particles and no attempt was made to alkaline age the samples. BET surface area measurements on the dried silica samples were always found to be almost exactly what was reported by the colloid manufacturer, indicating that the original primary particles still existed intact in the gel structure, without significant coalescence. All were impregnated with 0.35 Cr/nm^2, activated at 700 °C, and tested for polymerization at 105 °C. All samples made respectable amounts of polymer, even though the low surface area samples provided poor activity, as would be expected. Results are shown in Table 6.

Fig. 9 shows the pore size distributions from some of these catalysts. The colloidal particle size was varied from 7 up to 85 nm, according to the manufacturer's analyses. After gelation, the hydrogels were dried in different ways. Some were made by first replacing the pore water with alcohol, then drying the sample. In one case the alcohol was then replaced with isobutane liquid, which was heated in an autoclave to the critical point before venting. This tends to yield higher pore volumes because the surface tension approaches zero at the critical point. In other cases, the aqueous colloidal suspension was simply dried without gelation in a vacuum oven at 110 °C. Obviously this approach provided lowest PV. Notice that for each method of drying, the smaller colloidal particles (higher surface area) tended to resist the forces of dry-

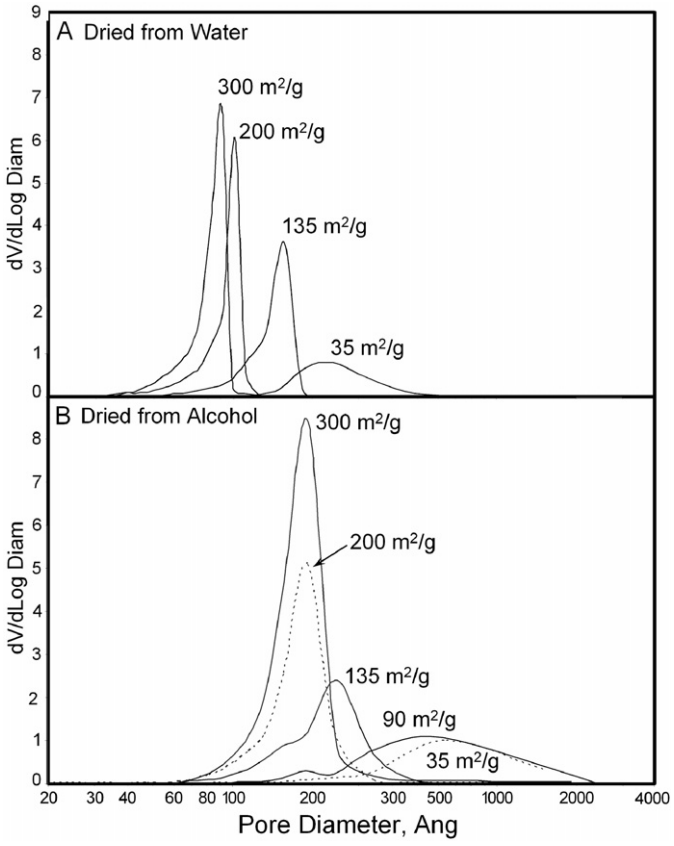

Fig. 9. Pore size distributions of silica gels derived from colloidal suspensions, dried containing either (A) water or (B) alcohol in the pores.

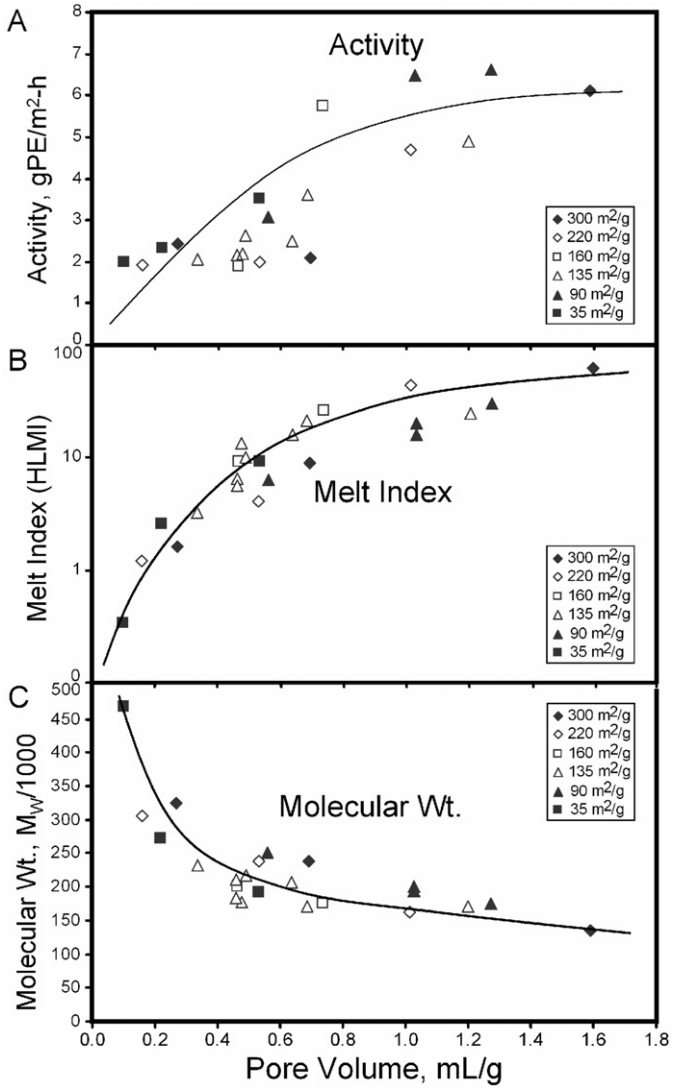

Fig. 10. Results of catalysts made from colloidal silicas varying in surface area. (A) Activity, (B) melt index, and (C) molecular weight, all plotted against pore volume.

ing better than the larger particles, yielding slightly higher PV. The reason for this is obscure. Perhaps the total number of particle contacts in the network plays a secondary role in determining the strength of the network. Notice also that the larger particles tended to produce larger pores, as would be expected for a similar coordination number. Obviously the holes between particles must be comparable in size to particle itself.

After drying with 0.35 Cr/nm^2 these catalysts were activated at 700 °C and tested for ethylene polymerization at 105 °C. The activity, after normalization by surface area, is plotted in Fig. 10A against pore volume. There is little correlation with pore diameter in this study, but when plotted in this way one can discern a dependence on pore volume, although with significant scatter. We interpret this to mean that the two variables may act independently. That is, while pore diameter may indeed important in letting polymer escape from fragments as was seen in the above studies, it is pore volume that mainly determines friability, and thus PV is of equal or in this case greater importance to the activity.

The friability of these non-reinforced silicas is probably related to the number of contacts between particles, and the strength of those contacts. The number of contacts each particle has with

Coordination Number		Solids Concentration vol%	wt%	Pore Volume mL/g
12		75%	87%	0.16
6		52%	70%	0.42
3		5%	10%	8.6
3-2-3		1.3%	2.8%	35
3-2-2-3		0.83%	1.8%	54

Scheme 2. Relationship between pore volume and average number of contacts between primary particles.

other particles is called the coordination number. It is the coordination number that determines the pore volume, and this relationship is independent of particle size, surface area, or pore diameter. Scheme 2 illustrates the connection [8].

Fig. 10B shows the melt index response of these samples to pore volume. All of these samples, regardless of the surface area (i.e. the primary particle size), formed a similar relationship, although admittedly with some scatter. The Y-axis is on a log scale to cover the wide range, but otherwise the curve is similar to that in Figs. 1 and 4. Fig. 10C plots the molecular weight obtained from these samples, again against pore volume. Once more a single relationship seems to have been formed, regardless of the primary particle size, very similar to that in Figs. 1 and 4. This suggests that the primary particle size, and consequently the radius of curvature or the surface area itself, is not fundamental to the dependence of molecular weight on porosity.

Thus, despite the wide variation in primary particle size used in this data set, it is the way the network is formed and dried that is the dominant variable. Pore volume seems to capture this best. It seems to be the pore volume, and not the pore diameter, or surface area, that provides the best correlation with activity, M_W and melt index. When plotted against surface area these data yielded no correlation. When plotted against pore diameter, these data yielded separate lines for each surface area, again demonstrating the role of PV. This is different from the reinforced samples in Figs. 5, 6 and 8, where pore diameter was used. In those studies, however, the PV was relatively higher and less varied than in this study. It is possible that fragmentation was less complete in this study, and therefore the gel strength was more important. Under these conditions the strength of the xerogel may somehow influence the polymer M_W as well as the activity.

The MW distribution from these silicas, shown in Fig. 11, exhibited the same trends noted earlier in Figs. 3, 7, and 8. As the PV decreased, a shoulder appeared on the high MW side of the MW distribution, developing into a second peak at very low PV. In this data set low PV usually also meant small pore diameter. However, unlike Fig. 8, there was no evidence here that a very large average pore diameter could yield the high MW peak. In Fig. 8 large pore

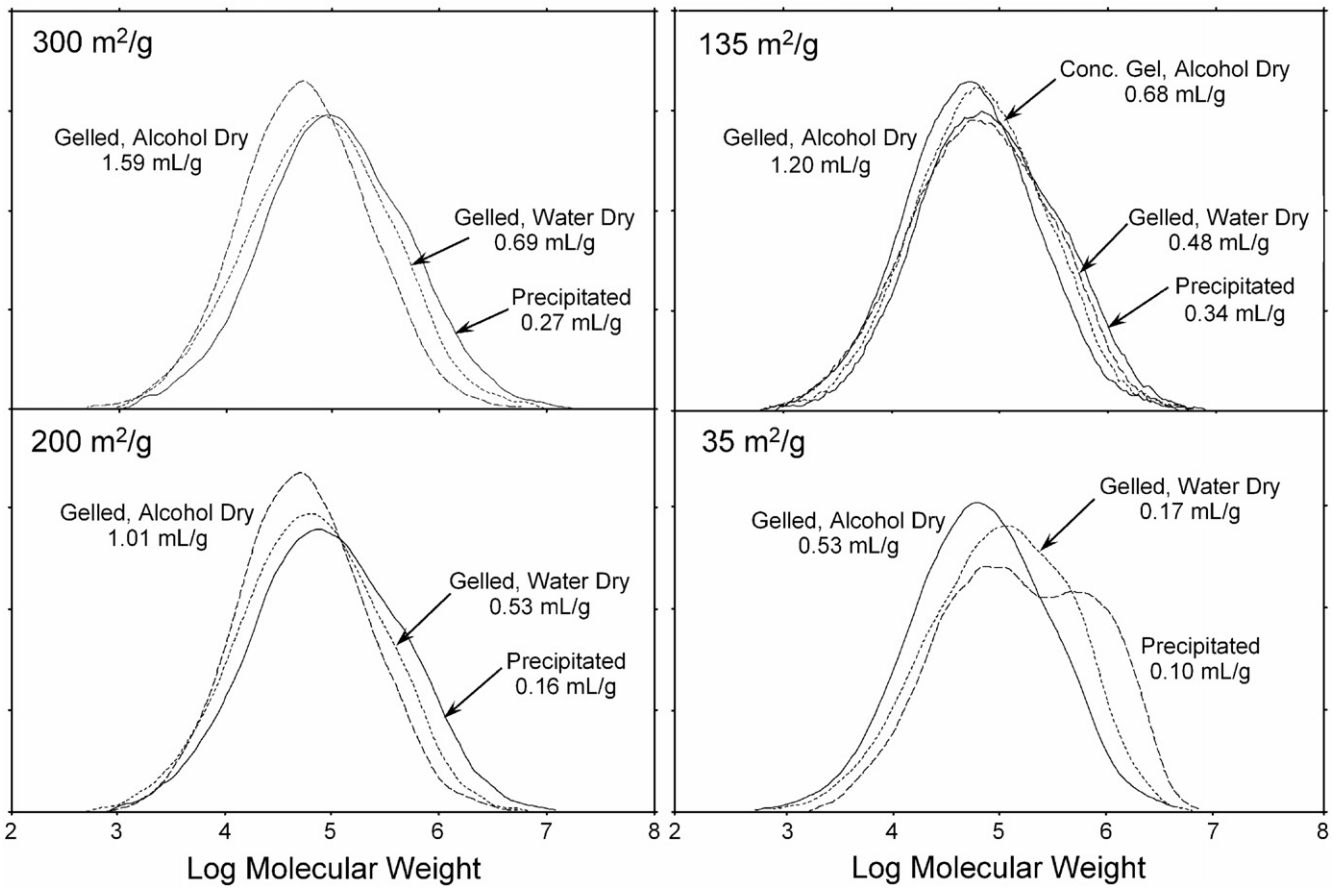

Fig. 11. MW distributions from colloidal silicas.

diameters were due to extreme reinforcement of the network, thus probably generating a very strong matrix. In contrast, in this set of data large pore diameters were the result of larger primary particles combined with high PV, and generally indicated a weakened structure.

3.8. Precipitated silicas

At the bottom of each section in Table 6 the silica samples were made by a slightly different technique. Instead of gelling the different colloidal suspensions by pH adjustment, they were instead simply dripped into a large volume of isopropyl alcohol. This caused a fine flocculent precipitate to settle out of the alcohol. Although these precipitates were made from the same colloidal particles as the other samples, the final dried catalysts behaved quite differently. As a rule they produced much higher molecular weight (lower melt index) polymer than the corresponding gels of similar PV.

The total pore volume from these precipitates was usually quite respectable, which at first seems inconsistent with their behavior. The PV distribution, however, reveals a somewhat different picture. The distribution is bimodal, with some very large pores that contain most of the volume, and some very small pores where most of the area resides. Fig. 12A shows the pore volume distribution from these precipitated colloidal silicas of different surface areas. One can see the bimodal distribution, and that most of the volume is in the larger pores. In contrast, Fig. 12B shows the surface area distribution. Now the small into a larger structure. The process is illustrated in Scheme 1D. The small pores come from *within* the aggregates, while the large pores measure space *between*

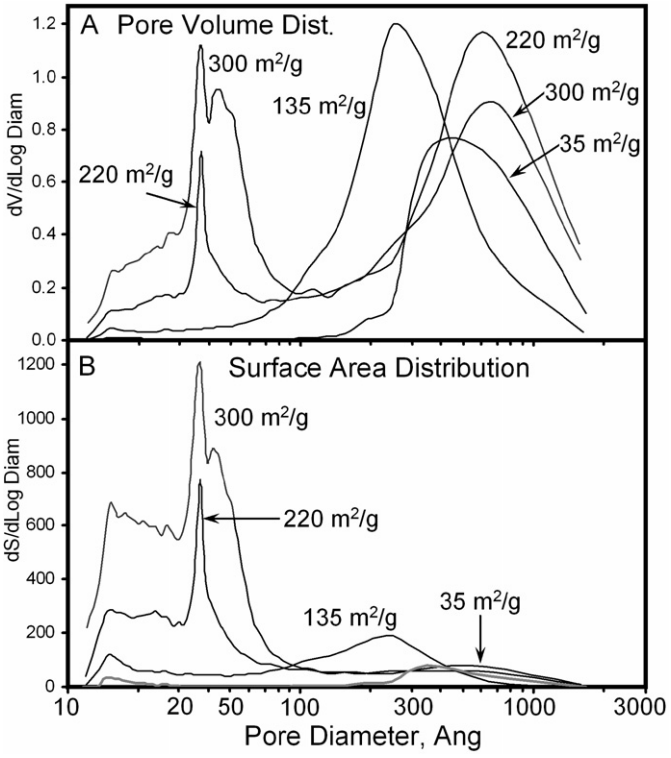

Fig. 12. (A) Pore volume and (B) surface area distribution of catalysts made by precipitation of colloidal silicas.

Table 7
Results from Sylox and two precipitated silicas from W.R. Grace.

Silica grade (W.R. Grace)	Surface area (m^2/g)	Pore volume (mL/g)	Avg. pore diameter (Å)	Area in pores <40 Å (%)	Activity per nm^2 (gPE/m^2-h)	Molecular weight (M_W/1000)
Sylox 100A	257	1.43	222	0%	4.4	167
Sylox HSA	226	1.91	337	2%	7.8	233
Sylox 200A	147	1.67	454	13%	11.4	219
Sylox 300A	137	1.81	530	12%	11.0	238
Sylox 2	117	1.07	366	24%	10.7	230
Sylox SD	105	1.59	606	14%	9.8	189
Precipitated SM500	102	1.07	420	26%	13.2	240
Precipitated SM660	169	2.05	485	20%	10.8	157

the aggregates. Obviously most of the area resides in the smaller pores.

Therefore most of the active sites are inside the small pores. If one only counts the volume within the small pores, then the precipitated catalysts seem to behave like their gelled counterpoints. In Table 6, and in Figs. 10 and 11, the PV used is that volume which accounts for 90% of the surface area. This adjustment merges the precipitate and gel data nicely, indicating that they obey a similar behavior, and that it is this small pore volume that is most important. In Fig. 10 it is clear that these small pores have the expected influence on the MW distribution.

In one experiment in Table 6 the precipitated silica was then given an 80 °C aging step in NH_4OH solution before drying. This treatment did not change the surface area significantly, but it did apparently strengthen the matrix enough to yield a slightly higher PV after drying. This, in turn, then influenced the polymer molecular weight as before.

Many grades of precipitated silicas are available from commercial silica manufacturers that are used for rubber and plastics reinforcement, cosmetics, and many other uses. They are generally known for having large pores. Two grades were obtained from W.R. Grace to test in this survey of silica types. The results are shown at the bottom of Table 7. Although both grades had low surface area, the total pore volume measured by nitrogen sorption was quite respectable, with most of the volume inside 800–900 Å pores. However, the pore size distribution also included many small pores, and the area was distributed within the entire pore range. Table 7 also shows the percentage of area inside pores smaller than 40 Å.

The activity from both precipitated silicas, plotted in Fig. 13A, was quite high, perhaps due to the very open structure. The molecular weight, plotted in Fig. 13B, is fairly low, especially the high PV sample. These commercial precipitated silicas tended to produce the same high MW shoulder in the MW distribution. This is shown in Fig. 14A. Grade Sylopol SM500, the lower porosity of the two, yielded the most noticeable high MW shoulder.

3.9. Sylox grade silicas

W.R. Grace manufactures an unusual grade of silica under the name of "Sylox." These silicas (there are several variations within the Sylox grade) are also distinguished from typical silica gels in having extremely large pores. The pore volume is high, but not unusual for polymerization grade silicas. Rather it is the surface area that is especially low, resulting in a large average pore diameters. Although the details of Sylox preparation are proprietary, Grace personnel describe it as "hybrid" between gelled and precipitated silicas, and the word "reinforced" is used, perhaps as in a secondary deposition of silica. Thus, in a survey of silica types, Sylox offers a unique opportunity to test large pore silica of relatively high pore volume.

Table 7 lists the properties of several Sylox grade silicas, after having been converted into catalysts and activated at 700 °C. Pore

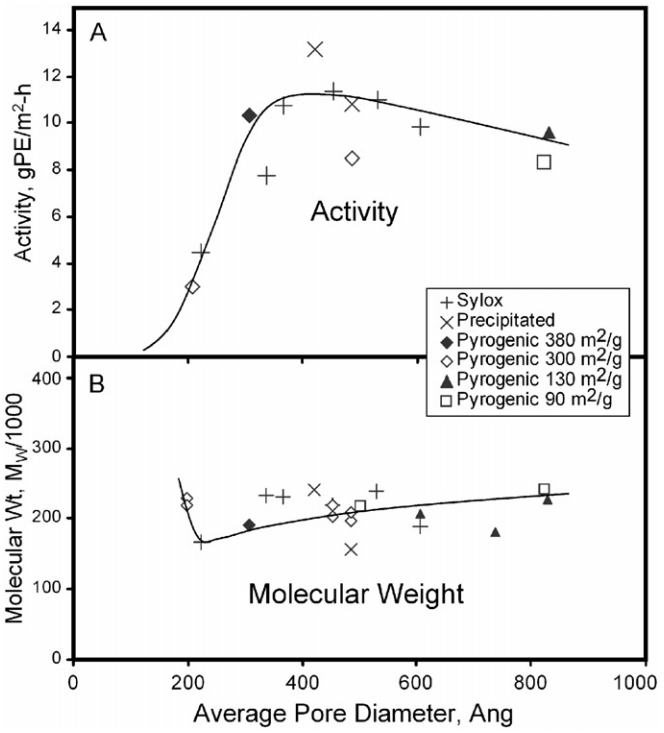

Fig. 13. Results from Sylox, precipitated, and pyrogenic silicas showing (A) activity and (B) molecular weight, each plotted against pore diameter.

volumes range from 1 to 2 mL/g and surface areas from 250 down to 100 m^2/g. This combination yields average pore diameters up to 600 Å. Fig. 15A shows the PV distribution of these silicas. Again there is evidence for a range of pore sizes, with most of the volume inside the very largest pores, but with the area more evenly dispersed. Table 7 also lists the fraction of area inside pores less than 40 Å.

The activity of the Sylox grades, after normalization for surface area is plotted in Fig. 13A. It increased with average pore diameter reaching a high plateau by about 350 Å. Since the total pore volume was relatively high and unchanged within this series, this again suggests that the pore radius may be important in itself, perhaps promoting polymer escape from within the fragments. In fact the shape of the activity response is much like that in Figs. 5, 6 and 8, only perhaps shifted to slightly higher diameters. This small shift may be due to the very wide pore distribution. Unlike the precipitated bimodal examples in Table 6, no correction was applied here to compensate for the tendency of the smaller pores to contain disproportionately more area.

The molecular weight obtained from Sylox silicas can also be seen in Table 7. The lowest M_W was obtained at the lowest average pore diameter of 222 Å. This was considered near the optimum

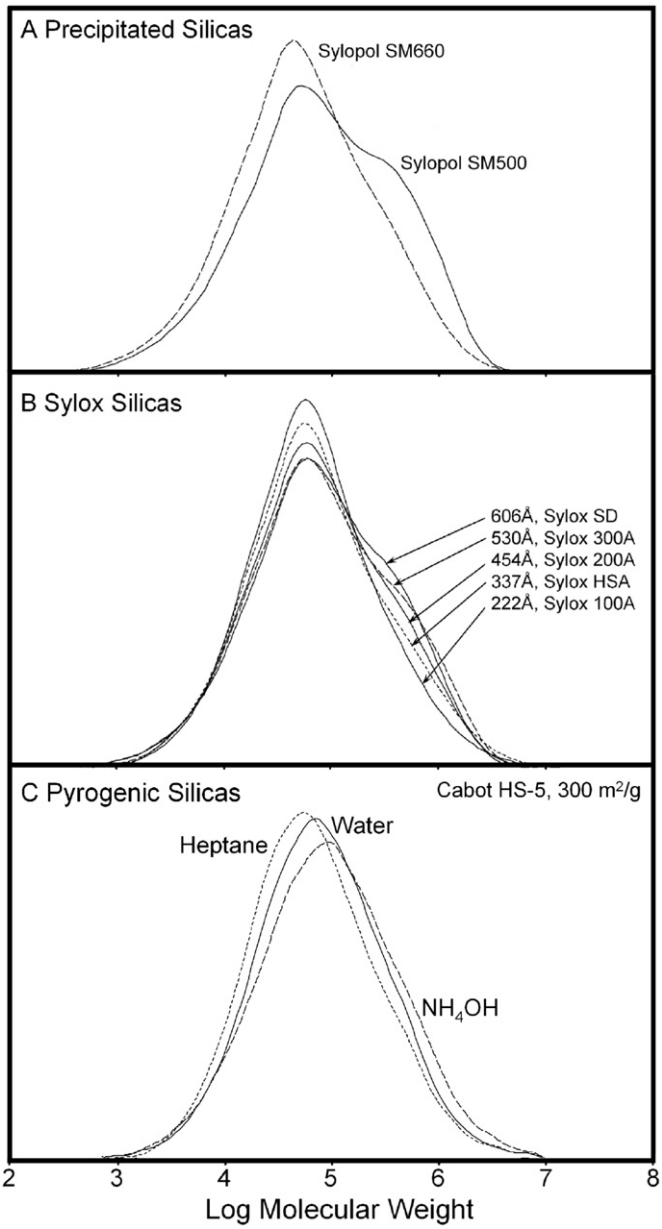

Fig. 14. MW distribution from (A) precipitated, (B) Sylox, or (C) pyrogenic silicas, all from W.R. Grace or Cabot.

diameter for other reinforced silicas as in Figs. 5, 6 and 8. Fig. 13B plots the M_W against pore diameter. The Sylox curve is relatively flat. Perhaps this is because the Sylox silicas still retained their high PV even at large diameters, in contrast to the sintered samples.

The same high MW shoulder appeared on the MW distribution from Sylox silicas as the pore diameter was increased. This is shown in Fig. 14B.

3.10. Pyrogenic silicas

Fumed silicas are made by the vapor phase hydrolysis of $SiCl_4$ and other silanes in a hydrogen flame. They provide a unique structure in that chains or small aggregates of primary particles are formed independently, and not as part of a larger network [19–25]. Therefore pyrogenic silicas are fine, feathery, almost smoke-like powders, having extremely low bulk density. Depending on flame conditions the particles can be formed as individuals, or in chains

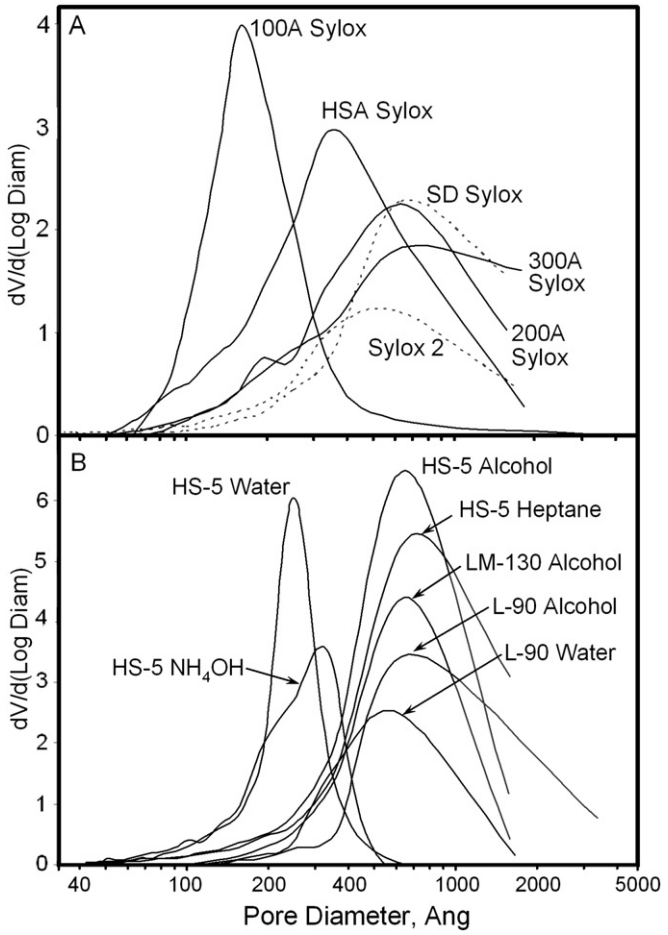

Fig. 15. Pore volume distribution curves from (A) W.R. Grace Sylox grade silicas and from (B) Cabot pyrogenic silicas dried from various solvents.

up to 200 nm long, or in small 3-dimensional aggregates of a few primarily particles. The degree of fusion between primary particles, i.e. the neck size, can vary considerably with flame temperature. Hot flames, and long residence times, tend to favor more highly fused materials with lower surface area. These pyrogenic silicas offer a chance to study the effect of silicas that already exist as small independent particles, and thus not having the usual pore structure.

Initially one could argue that these materials have no pore volume, or at least contain extremely large pores, which are really spaces between aggregates. To make catalyst from these commercial silicas, four grades were obtained from Cabot, varying in surface area from 400 to 90 m^2/g. These were impregnated with chromium using a gas phase technique, or a solvent of heptane, alcohol, or water. Evaporation of the solvent did cause some shrinkage of the natural structure, although the pore size was still quite respectable for all samples. When dried from heptane or alcohol, PV $>$ 3 mL/g was sometimes possible. These pyrogenic catalysts were then activated at 700 °C and tested for polymerization activity. Table 8 lists catalyst properties and polymerization results. The pore volume distribution from these samples, shown in upper Fig. 15B, is dominated by large pores.

First, it should be noted that the pyrogenic silicas, despite their lack of the usual gel; network structure, were not found to be more active than silica gels of equivalent surface area. This was true even of the samples where vapor phase Cr deposition was used. Since all surface is presumably exposed on those pyrogenic samples, without the need for fragmentation, this suggests that (when

Table 8
Results from pyrogenic silicas.

Cabosil grade	Dried from	Surface area (m^2/g)	Pore volume (mL/g)	Avg. pore diameter (Å)	Molecular weight (M_w/1000)
EH-5	Alcohol	380	2.91	306	192
HS-5	Heptane	296	3.60	486	198
HS-5	Heptane	296	3.60	486	208
HS-5	Alcohol	275	3.12	454	218
HS-5	Alcohol	275	3.12	454	204
HS-5	Water	282	1.40	198	229
HS-5	Water	282	1.40	198	218
LM-130	Alcohol	124	2.58	830	227
LM-130	Alcohol	129	1.96	607	206
LM-130	Alcohol	123	2.26	737	181
L-90	Acetone	92	1.89	824	242
L-90	Water	89	1.12	502	216
HS-5	NH_4OH	241	1.25	207	265
L-90	Sonicated, H_2O	95	1.40	588	273

made correctly) silica gels also fragment down to the point where all or most of the surface is available [1].

Fig. 13B plots the molecular weight obtained from the pyrogenic silicas against average pore diameter. They are mostly low, and fairly independent of pore volume or pore diameter—much as one might expect from free non-fragmenting particles. The exact pyrogenic grade, which varied considerably in surface area, did not make much difference. This is another indication that the surface area itself is probably unimportant in determining molecular weight.

However, one can perhaps see a very slights dependence on pore volume. The 300 m^2/g samples made from HS-5, gave molecular weight that did vary slightly with drying method, and thus PV. Notice that when dried from water to produce a pore diameter of 198 Å, a slightly higher MW was obtained than when dried from heptane or alcohol. This suggests that some network formation may occur during drying, even for pyrogenic silicas.

There is also a very slight shift to higher M_W at very high pore diameters, which were from the lower surface area grades, LM-130 and L-90. This may indicate some low-level structure that has been fused into the aggregates of these two materials.

The MW distribution from all of these pyrogenic silicas was nearly uniform. Only a very slight tendency to produce the high MW shoulder was observed with pore volume, as noted in o other series above. An example is shown in Fig. 14C where the 300 m^2/g grade HS-5 silica was wet and then dried from three different solvents.

In two experiments in Table 8 an attempt was made to cement the pyrogenic particles into a more firm pseudo-network, thus increasing their strength. First, HS-5 was combined with ammonium hydroxide to make a paste, then it was dried from that solution. A lower surface area and pore volume resulted, indicating that some particle fusion from alkaline aging may have occurred. This material gave higher M_W despite the similar pore diameter. The MW distribution, shown in Fig. 14C, also broadened on the high MW side. In the second experiment, L-90 was sonicated in water for an hour under very high power in order to break up some of the structure. Then the silica was dried and activated. The pore volume was respectable, at 1.4 mL/g, but this material still produced higher M_W polymer. The treatment also enlarged the high MW shoulder on the MW distribution. In both experiments, the response suggests a correlation with the strength of the network structure.

3.11. Molecular sieves

The broad MW distribution obtained from Cr/silica is usually attributed to site heterogeneity resulting from the amorphous silica surface. Molecular sieves are a crystalline form of silica, potentially offering a more uniform environment for the Cr. Thus it is of interest to observe the MW distribution from such materials. A number of studies have been reported on Cr supported by molecular sieves, and although none has addressed this question in particular, a few did note that a broad MW distribution was obtained [26–30]. We also tested several molecular sieves as part of this survey, and the results are summarized in Table 9. We found no evidence for single-site behavior or even a more uniform environment. The MW distributions from these materials were quite broad, like that from amorphous silica.

Molecular sieves are noted for their acidity, in contrast to pure silica. These materials exhibited no activity under these conditions in the absence of chromium. However, one could still argue that such acidity could affect the chromium. Therefore we chose molecular sieves that were not acidic (HMS, i.e. hexagonal mesoporous silica, from Aldrich), possessed low acidity (MCM-41 from Aldrich), or were washed in nitric acid to remove aluminum ions (mordenite, types A and Y). It is also worth noting that the effect of acidity on the Phillips catalyst is a low MW shoulder on the distribution, very slight in comparison to the changes observed here [1]. We saw no evidence of such changes from these molecular sieves.[4]

To protect their structure these molecular sieves were only calcined at 400–500 °C. Only type A was activated at the usual 700 °C. This influences the activity, and especially the molecular weight, which was generally higher than in studies above, with the exception of the type A sample.

The micro-framework of molecular sieves is quite different from the macro-structure of silicas, and one might expect different fragmentation behavior. We obtained minimal activity from all samples with the exception of the hexagonal mesoporous silica (HMS), which was also low in comparison to 500 °C silica. Nevertheless

[4] In fact Cr attached to acidic sites seems to be thermally unstable. On Al modified silica the low MW shoulder diminishes and disappears between 400 and 700 °C.

Table 9
Results from molecular sieves.

Molecular sieve	Peak pore diameter (Å)	Surface area (m^2/g)	Pore volume (mL/g)	Avg. pore diameter[c] (Å)	Activity (gPE/m^2-h)	Molecular weight (M_W/1000)
Acid washed mordenite	7[a]	530	0.17	13	0.1	412
HNO_3 leached zeolite Y	7–13[a]	545	0.21	15	0.1	576
Type A	4–11[a]	534	0.22	16	0.1	395
MCM-41	25[b]	1090	1.16	43	0.1	422
Hexagonal mesoporous	36[b]	742	2.31	125	0.9	553

[a] From known structure.
[b] From N_2 sorption.
[c] From 4PV/SA.

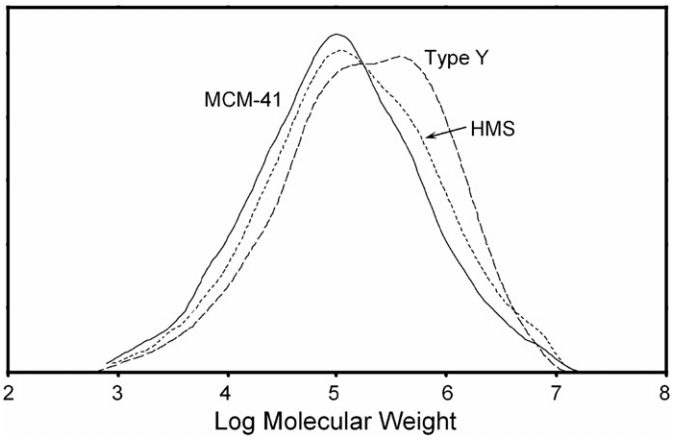

Fig. 16. MW distribution obtained from various molecular sieves.

enough polymer was obtained, probably escaping from very shallow depths near the particle exterior, from several of them to analyze. The two meso-porous materials had peak pore diameters of 26 and 35 Å respectively. All these materials produced very high M_W, as might be expected from the narrow pore diameter and/or low PV. They also tended to produce the high MW shoulder on the MW distribution. That of H-mordenite and Y-zeolite might even be described as bimodal. Fig. 16 shows some of the MW distributions obtained.

4. Conclusions

The molecular weight obtained from Cr/silica catalysts is heavily influenced by its porosity. However, this response does not correlate with any one physical measurement, such as surface area, radius of surface curvature, pore volume, or pore diameter. In some cases pore volume seems to correlate, while in others it is the pore diameter that fits best, as first reported by Hogan [6]. Neither is the MW response due to enhanced dehydroxylation during activation, as was demonstrated by the compaction experiments.

Rather, all these studies together suggest that two properties could be contributing independently to the observed responses. The participation of the surface inside a fragment depends on (1) the fragment size, and (2) the depth from which polymer may escape. The former might be controlled largely by the pore volume and the latter by the pore diameter. We suggest that polymer made inside tightly packed pores may grow to higher MW than that made on the fragment's exterior.

It has been assumed that the interior of fragments cannot contribute to the observed activity, since the pores very quickly become plugged with polymer [31]. Certainly this can sometimes be true, since low PV silicas that do not fragment are inactive. However, there may be a certain limited depth below the fragment exterior from which polymer can still escape and thus contribute. If this were not so, it would be hard to explain why the silica porosity influences so many polymer properties. In addition to M_W and MW distribution, which have been detailed in this report, the silica porosity also influences the amount of long chain branching [1,32], to be described in a future report, and comonomer incorporation [33].

Therefore, first, the pore volume largely controls the fragility of the catalyst, which determines the degree of fragmentation and thus the fragment size. This may explain the activity and MW dependence on PV in Figs. 1, 4 and 10. In Fig. 10 the pore diameter varies independently of PV, but it did not correlate with MW, which indicates the importance of PV itself.

Secondly, the depth from which polymer can escape probably depends on the pore diameter. This is very clear in Fig. 5 where the PV remained constant, and also in Fig. 6 where the PV change was not large. Large pore catalysts often provided full activity even when the pore volume was not high, as in Figs. 6 and 8. The molecular weight often increased with coalescence to yield larger pores. That increase can be major if the PV also shrinks, producing the V-shaped curve in Figs. 6 and 8. Or it can be flat if the PV remains high, as in Fig. 13. The optimum pore diameter for activity and molecular weight was around 200–300 Å. Again there is evidence that polymer made inside tightly packed pores may grow to higher molecular weight.

Thus high pore volume tends to produce smaller fragments, and polymer can escape from the interior more easily through large pores. These two opposing trends determine, not only the shape of the MW response to pore diameter, but also the characteristic bimodal MW distribution. Presumably the low MW peak comes from polymer made on the surface of fragments, and the high MW peak from the interior.

Exactly why polymer made inside pores should grow to higher molecular weight is unclear. Ethylene diffusion into the pore structure would predict the opposite behavior. Since molecular weight and activity (per square meter) often responded similarly, it is tempting to blame localized overheating for the MW change. However, Fig. 8 contradicts this. Also, other variables like poisons or Cr loading influence activity, but do not yield the expected MW response. So at present the mechanism is unknown.

Finally, this paper has dealt only with Cr/silica catalysts. One might ask how widely the principles observed here apply to other catalyst systems. We know that amorphous aluminophosphate supports (where P/Al > 0.4) obey these same trends when chromium is added. We also know that Cr on layered clay does not follow the same trends. Given the different structure of gamma alumina, which is composed of micro-crystallites, it seems likely that its dependence on porosity would also be different. Actually, Cr/alumina produces such high MW that it is difficult to faithfully conduct a test. Supported Ziegler catalysts are also difficult to test with accuracy because they produce ultrahigh MW PE in the absence of hydrogen.

Metallocenes are also difficult to study in this context because hydrogen is continuously generated with polymerization and the MW can significantly change during the run. For an accurate evaluation of porosity, that fact must be taken into account. Metallocenes present another difficulty because the silica is usually impregnated with methylaluminoxane, which is as big a molecule as the pores being studied, and the loadings are usually far above a monolayer, even if the MAO could penetrate. Therefore it is likely that much of this type of catalyst is actually outside of the pores of the silica. It is hoped that the use of solid acid activators, such as those developed in this laboratory during the 1990's [34], may overcome this limitation in future studies.

References

[1] M.P. McDaniel, in: G. Ertl, H. Knozinger, F. Schuth, J. Weitkamp (Eds.), Handbook of Heterogeneous Catalysis, second ed., Wiley–VCH, Weinheim, 2008, pp. 3733–3792, chap. 15.1.
[2] M.P. McDaniel, Adv. Catal. 33 (1985) 47–98.
[3] J.P. Hogan, J. Polym. Sci. Part A-1 8 (1970) 2637.
[4] J.P. Hogan, D.D. Norwood, C.A. Ayres, J. Appl. Polym. Sci. 36 (1981) 49–60, ISSN:0271-9460.
[5] C.E. Marsden, in: V.E.G. Poncelet, P.A. Jacobs, P. Grange, D. Delmon (Eds.), Studies in Surface Science and Catalysis, vol. 63, Preparation of Catalysts V, Elsevier, Amsterdam, 1991, pp. 215–227.
[6] J.P. Hogan, A.G. Kitchen, Controlling the melt index of poly-1-olefins, US Patent 3,225,023, issued December 21, 1965 to Phillips Petroleum Co.
[7] E.M.E. van Kimmenade, J. Loos, J.W. Niemantsverdriet, P.C. Thüne, J. Catal. 240 (2006) 39–46.
[8] R.K. Iler, The Chemistry of Silica: Solubility, Polymerization, Colloid and Surface Properties, and Biochemistry, Wiley, New York, 1979, 886 pp.

[9] M. Einardsrud, L. Rormark, S. Haereid, T. Grande, J. Non-Cryst. Solids 211 (1997) 49–55.
[10] V.A. Dzisko, A.A. Vishnevskaya, V.S. Chesalova, Zh. Fiz. Khim. 24 (1950) 1416.
[11] C.J. Brinker, G.W. Scherer, Sol–Gel Science, Academic Press, San Diego, CA, 1990.
[12] I.S. Chuang, G.E. Maciel, J. Phys. Chem. B 101 (1997) 3052–3064.
[13] W.A. Patrick, US Patent 1,297,274 issued March 18, 1919 to W.R. Grace Company.
[14] G.A. Ellsworth, US Patent 3,526,603 issued September 1, 1970 to W.R. Grace Company.
[15] H.E. Ries, Advances in Catalysis and Related Subjects, vol. 4, Academic Press, New York, 1950, p. 87.
[16] Kirk–Othmer Encyclopedia of Chemical Technology, vol. 21, fourth ed., Wiley, ISBN 0-471-52690-8, 1997, 977 pp.
[17] M.P. McDaniel, D.R. Witt, E.A. Benham, J. Catal. 176 (1998) 344–351.
[18] D.R. Witt, E.A. Benham, M.P. McDaniel, Controlled addition of alkali or alkaline earth salts to a chromium oxide catalyst, US Patent 5,444,132, August 22, 1995, Assigned to Phillips Petroleum Co.
[19] J.E. Martin, D.W. Schaefer, A.J. Hurd, Phys. Rev. A 33 (5) (1986) 3540; J.E. Martin, D.W. Schaefer, A.J. Hurd, Phys. Rev. A 35 (5) (1987) 2361.
[20] S.E. Pratsinis, Prog. Eng. Combust. Sci. 24 (1998) 197.
[21] S. Tsantilis, S.E. Pratsinis, Langmuir 20 (2004) 5933–5939.
[22] R. Mueller, H.K. Kammler, S.E. Pratsinis, A. Vital, G. Beaucage, P. Burtscher, Powder Technol. 140 (2004) 40–48.
[23] J.H. Lee, G. Beaucage, S.E. Pratsinis, S. Vemury, Langmuir 14 (1998) 5751–5756.
[24] R. Wengeler, A. Teleki, M. Vetter, S.E. Pratsinis, H. Nirschl, Langmuir 22 (2006) 4928–4935.
[25] R. Wengeler, F. Wolf, N. Dingenouts, H. Nirschl, Langmuir 23 (2007) 4148–4154.
[26] B.M. Weckhuysen, R.R. Ramachandra, J. Pelgrims, R.A. Schoonheydt, P. Bodart, G. Debras, O. Collart, P. Van der Voort, E.F. Vansant, Chem. Eur. J. 6 (16) (2000) 2960–2970.
[27] Y. Zhang, I. Matos, M. Lemos, F. Freire, T. Nunes, A. Botelho do Rego, R.T. Henriques, F. Fonseca, M. Marques, F. Lemos, J. Polym. Sci. Part A Polym. Chem. 41 (2003) 3768–3780.
[28] G. Calleja, J. Aguado, A. Carrero, J. Moreno, in: J. Cejka, N. Zilkova, P. Nachtigall (Eds.), Studies in Surface Science and Catalysts, vol. 158, Elsevier, 2005, p. 1453.
[29] G. Calleja, J. Aguado, A. Carrero, J. Moreno, Appl. Catal. A 316 (2007) 22–31.
[30] Y. Zhang, X. Wang, M.A.N.D.A. Lemos, F. Lemos, R.T. Henriques, M.M. Marques, in: G. Froment, K.C. Waugh (Eds.), Studies in surface Science and Catalysts, vol. 133, Science, 2001, p. 173.
[31] D.A. Estinoz, M.G. Chiovetta, Polym. Eng. Sci. 36 (17) (1996) 2208–2228, and 2229–2240.
[32] M.P. McDaniel, D.C. Rohlfing, E.A. Benham, Polym. React. Eng. 11 (2) (2003) 101–132.
[33] P.J. Deslauriers, M.P. McDaniel, J. Polymer Sci. 45 (15) (2007) 3135.
[34] M.P. McDaniel, J.D. Jensen, K. Jayaratne, K.S. Collins, E.A. Benham, N.D. McDaniel, P.K. Das, J.L. Martin, Q. Yang, M.G. Thorn, A.P. Masino, in: J.R. Severn, J.C. Chadwick (Eds.), Tailor-Made Polymers, vol. 7, Wiley–VCH, Weinheim, ISBN 978-3-527-31782-0, 2008, 171 pp.